Early taphonomy of benthic foraminifera in Storfjorden 'sea-ice factory': the agglutinated/calcareous ratio as a proxy for brine persistence

Maria Pia Nardelli, Eleonora Fossile, Olivier Péron, Hélène Howa, Meryem Mojtahid

BOREAS An international journal of Quaternary research

Early taphonomy of benthic foraminifera in Storfjorden 'sea-ice factory': the agglutinated/calcareous ratio as a proxy for brine persistence

MARIA PIA NARDELLI, ELEONORA FOSSILE, OLIVIER PÉRON, HÉLÈNE HOWA AND MERYEM MOJTAHID

BOREAS

Nardelli, M. P., Fossile, E., Péron, O., Howa, H. & Mojtahid, M.: Early taphonomy of benthic foraminifera in Storfjorden 'sea-ice factory': the agglutinated/calcareous ratio as a proxy for brine persistence. *Boreas*. https://doi.org/10.1111/bor.12592. ISSN 0300-9483.

The recurrent latent-heat polynya characterizing Storfjorden (Svalbard, Norway) triggers seasonal formation of thin first-year sea ice. This leads to the production of dense, salty, and corrosive brines that cascade towards the sea floor and mix with shelf waters. The bottom topography of the fjord is responsible for the retention of these dense waters in two central deep basins throughout the year. Recent studies show that living benthic foraminifera in Storfjorden are particularly affected by the persistence of brines on the sea floor, with a strong dominance of agglutinated (A) species and high degrees of dissolution of calcareous(C) faunas. Therefore, the A/C ratio, calculated on living faunas, was proposed as a proxy for brine persistence. In the present study we analyse the fossil faunas, found below the taphonomically active zone, to investigate the residual signal of the A/C proxy after the intense early taphonomic processes and challenge its applicability in sedimentary archives. Our results show that despite the generally high taphonomic loss inside the fjord, a high proportion of agglutinated species is still visible in fossil faunas at the stations experiencing regular and/or persistent presence of brine-enriched shelf waters. These results support the application of the A/C ratio in historical records to reconstruct the persistence of brines and indirectly the first-year sea ice formation in Storfjorden. This can be further applied to other Arctic fjords with similar settings and characterized by the production of brines during the winter–early spring season.

Maria Pia Nardelli (mariapia.nardelli@univ-angers.fr), Eleonora Fossile, Hélène Howa and Meryem Mojtahid, LPG UMR CNRS 6112, Université d'Angers, Nantes Université, Le Mans Univ, 2 bd Lavoisier 49045, Angers CEDEX 01, France; Olivier Péron, SUBATECH, UMR 6457, CNRS-Université de Nantes, 4 rue A. Kastler, 44307 Nantes, France; *received 7th January 2022, accepted 30th March 2022.*

The global ocean thermohaline circulation depends on the formation of deep waters in the Polar Regions. In the Arctic, deep waters are mainly formed by the densification of surface waters through cooling and salinity increase due to brine release in sea-ice production areas (e.g. Rudels & Quadfasel 1991). Storfjorden, in the Svalbard archipelago, is a major supplier of brine-enriched shelf waters, accounting for up to 5–10% of dense water production in the Arctic Ocean (Quadfasel *et al*. 1988; Smedsrud *et al*. 2006).

The release of brines is strictly related to the production of sea ice (Rysgaard *et al*. 2011) and therefore indirectly connected to climate forcings. The polynya regions (i.e. sea-ice free areas formed and maintained by advection of ice by offshore winds and currents) are the main zones where the production of brines occurs. Due to their largely ephemeral nature, polynyas have been suggested as sentinel regions for large-scale climate-related temporal sea-ice changes in polar marine environments (Smith & Barber 2007). There is solid evidence that ongoing climate change is strongly affecting sea-ice growth and extension in the Arctic (e.g. Meredith *et al*. 2019) and in this context the vulnerability of polynyas has been highlighted by several studies (e.g. Vincent 2019; Ribeiro *et al*. 2021). Among other possible consequences, the reduction of first-year sea-ice production in polynyas could lead to reduced brine-enriched shelf water (BSW) production with potential consequences for global deep-water circulation (e.g. Ohshima *et al*. 2016). The high natural variability of sea-ice dynamics in polynya regions, however, complicates long-term prediction based on direct present-day observations, acquired from satellite images. The main challenge is to understand the significance of the observed present-day sea ice trends on longer time scales (i.e. hundreds of years) to accurately predict their potential consequences for global ocean circulation.

The availably of only short-term information about interactions between the climate, the cryosphere and the oceans has motivated the development and calibration of geochemical and biological tracers preserved in sediments. These proxies are useful tools for historical reconstructions of sea-ice variability and marine environmental changes, on annual or multi-annual time scales (Limoges *et al*. 2018). Lately, several studies have been conducted to validate the application of proxies related to sea-ice dynamics, and several proxies seem suitable for tracing the presence and variability of sea ice i.e. dinoflagellate cysts, diatoms, ostracods, and biomarkers (see de Vernal *et al*. 2013 and references therein). However, each proxy presents some limitations (e.g. see review by de Vernal *et al*. 2013 for a complete overview), including the most promising ones that preserve well in recent sedimentary archives such as IP_{25} (organic lipid produced by sea-ice endemic diatoms) (Belt *et al*. 2007; Belt & Müller 2013; Belt 2018, 2019). For instance, the preservation and storage of the sediment samples for IP_{25} analyses are complex (Belt *et al*. 2007;

DOI 10.1111/bor.12592

Müller *et al*. 2009, 2011; Belt & Müller 2013) and some missing information further limits its applicability (e.g. absence of the biomarker in the Antarctic, (partially) unknown species responsible for the biomarker production, and the lack of knowledge about the distribution of those species in the Arctic region). All these aspects limit, at the moment, its application for sea-ice dynamics reconstruction in the northern Polar region. This further suggests the necessity of a multi-proxy approach to obtain reliable data sets for sea-ice reconstruction.

A previous investigation of benthic foraminiferal faunas under seasonal sea-ice cover conditions did not identify any endemic species exclusively related to sea-ice presence, and concluded that foraminiferal assemblages cannot be used as direct proxies for sea-ice cover (Seidenkrantz 2013). The recent study of Fossile *et al*. (2020), based on ecological interpretations from living assemblages in Storfjorden (Svalbard, Norway), suggested the potential use of a benthic foraminiferal-based proxy to reconstruct past brine production in coastal Arctic polynyas. Because the brine-enriched shelf waters cascading is directly related to first-year sea-ice growth (e.g. Skogseth *et al*. 2004, 2005a, 2008) the proposed proxy has been suggested as indirect indicator of seasonal sea-ice production (Fossile *et al*. 2020). This proxy, based on benthic foraminiferal assemblages, consists of the ratio between agglutinated (A) and calcareous (C) species, with the A/C ratio increasing in the presence of persistent brines at the sea floor (Fossile *et al*. 2020). Indeed, due to the CO_2 release during sea-ice formation and the interruption of direct exchanges with the atmosphere during winter, the brines are CO_2-enriched and consequently corrosive (Rysgaard *et al*. 2011), affecting therefore the mineralization of calcareous shells to the advantage of agglutinated forms. However, Fossile *et al*. (2020) also suggested that a high A/C ratio (i.e. high presence of agglutinated species) could also be related to high contents of quite refractory organic matter. Most probably, the combined effect of corrosive brines, organic matter remineralization, and persistence of brine-enriched shelf waters in the deep basins determine the dominance of agglutinated forms. In the deep basins, the organic matter is less labile, compared to the shallower stations where seasonal mixing and phytoplankton blooms favour fresher organic supplies to which calcareous species respond positively. A tolerance to less labile organic matter could be an additional competitive advantage for the agglutinated species inhabiting the fjord (Fossile *et al*. 2020).

Although promising, the possibility to realistically use the A/C proxy in historical records relies on: (i) the preservation potential of the agglutinated species dominating the living assemblages after death and below the taphonomically active zone (TAZ), corresponding to the bioturbated zone beneath the sediment surface where most early diagenesis occurs (Davies *et al*. 1989; Berkeley *et al*. 2007); and (ii) the preservation of the residual calcareous specimens after early dissolution events. In fact, agglutinated species, and in particular the species with organic cement, are known to be particularly fragile and to have a bad preservation potential in the fossil faunas (Bizon & Bizon 1984; Schröder 1988; Bender 1995). In Storfjorden, however, exceptional preservation of agglutinated foraminifera was reported from relatively recent fossil records (e.g. Late Holocene; Rasmussen & Thomsen 2014, 2015), probably promoted by low temperatures and high sedimentation rates. Therefore, their preservation in this region should ensure a good representativity of foraminiferal assemblages from historical sedimentary archives.

The aims of the present study are to: (i) estimate the information loss due to taphonomy of benthic foraminiferal assemblages and (ii) challenge the possibility of using the A/C ratio calculated from fossil faunas as a proxy for brine-enriched shelf water persistence in the recent past (tens to hundreds of years). The study of Fossile *et al*. (2020) investigated living assemblages in Storfjorden and provided ecological information about the main foraminiferal species. By comparing living assemblages from the topmost centimetres of sediment (Fossile *et al*. 2020) with dead and fossil foraminiferal assemblages from the same cores, we further investigate in the present study the preservation state of foraminiferal assemblages from fossil faunas just below the TAZ and the effect of taphonomic processes on the residual assemblages.

Material and methods

Study area

Storfjorden is the largest fjord of the Svalbard archipelago, Norway (latitude 74°N–81°N, longitude 10°N–35°E, Fig. 1). The oceanography of the Svalbard archipelago is influenced by two major water-masses: cold and relatively low saline Arctic waters, flowing out from the Barents Sea via the East Spitsbergen Current (ESC), and warm and saltier Atlantic waters, carried northwards through the Fram Strait by the West Spitsbergen Current (WSC) (Fig. 1; Loeng 1991). Cold Arctic waters, originating from the ESC, enter Storfjorden through its southern entrance, and form two passages in the northeast of the fjord head (Fig. 1; Skogseth *et al*. 2005b). These Arctic waters circulate as a coastal current in Storfjorden and exit the fjord along the southwest, successively flowing towards the North of Svalbard along the west Spitsbergen coast (Skogseth *et al*. 2005b). The Atlantic waters, originating from the WSC, occasionally inflow at intermediate water-depths in Storfjorden during the warm season (e.g. Skogseth *et al*. 2005a, b).

Located in the south of the archipelago, Storfjorden is characterized by shallow water depth in the innermost area (average depth ~100 m), two central deep basins

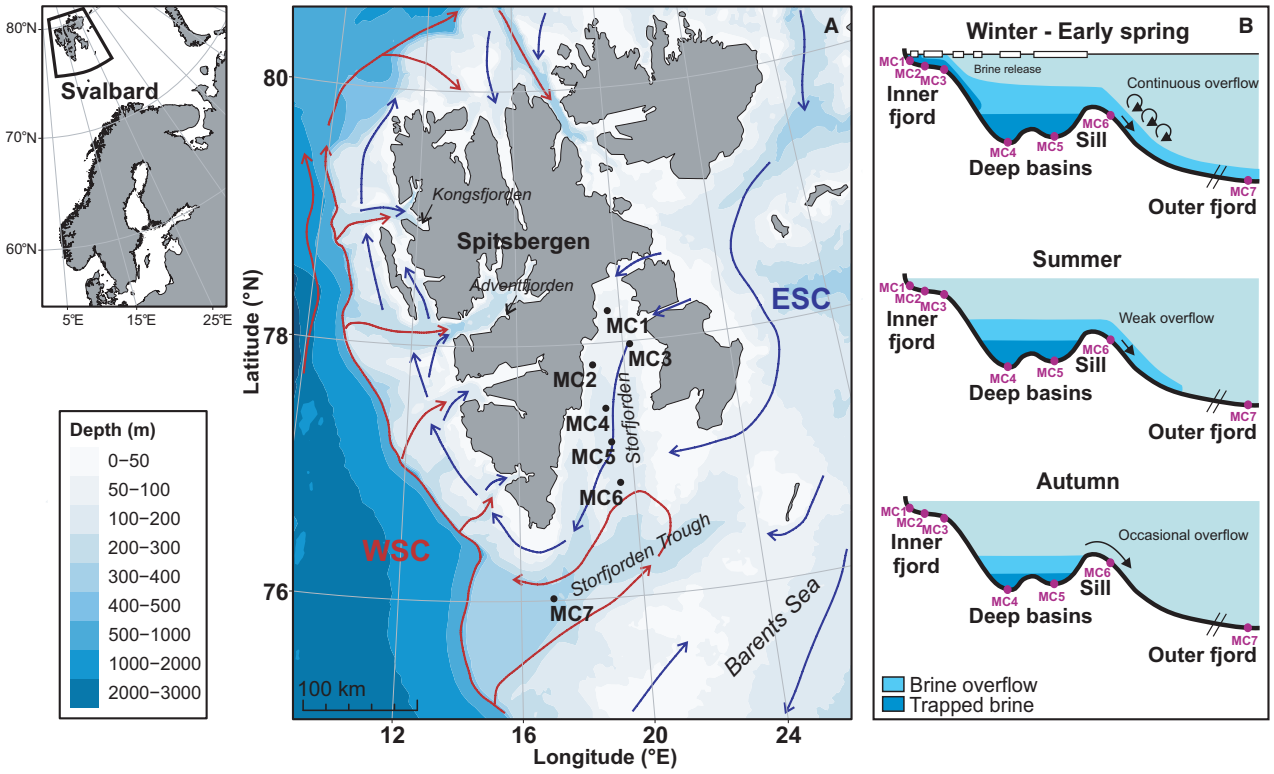

Fig. 1. A. Svalbard map with bathymetry showing the main currents influencing the archipelago and location of the seven sampling stations along an inner–outer transect in Storfjorden. Atlantic waters transported via the West Spitsbergen Current (WSC) are displayed in red, while the Arctic waters transported by the East Spitsbergen Current (ESC) are displayed in blue. The map was prepared with R package *PlotSvalbard* (Vihtakari 2020) using the R software environment (R Core Team 2020). B. Bathymetric profile sketches showing seasonal formation and flow of brine in Storfjorden (modified from Skogseth *et al.* 2005a; Rasmussen & Thomsen 2015; Fossile *et al.* 2020) and the indicative locations of the sampling stations (pink dots).

(average depth ~180 m) and a sill (~120 m water depth) that separates these basins from the outer shelf (>200 m). The inner part of Storfjorden is characterized by the presence of a latent-heat polynya, where thin first-year sea ice is continuously produced during winter–early spring (Skogseth *et al.* 2004, 2005a). The sea-ice production process leads to the ejection of CO_2 and salt and the formation of dense, cold, salty, and corrosive brines (Anderson *et al.* 2004; Rysgaard *et al.* 2011). These waters cascade towards the sea floor as brine-enriched shelf waters, mixing with shelf Arctic waters (Skogseth *et al.* 2005a, b).

During the cold seasons, brine-enriched shelf waters fill the deep basins up to the sill level and overflow towards the Barents Sea and the Fram Strait, passing below the Atlantic waters (Fer *et al.* 2003). During summer, when sea-ice production has ceased, brine overflow over the sill weakens in summer and stops in autumn, but residual brine-enriched shelf waters remain trapped in the deep central basins all year round (Haarpaintner *et al.* 2001a, c; Skogseth *et al.* 2005a; Fig. 1). The production of brine-enriched shelf waters and their properties (salinity and density) in Storfjorden depend on the polynya activity and position, which in turn is influenced by climate variability (i.e. North Atlantic Oscillation; Skogseth *et al.* 2004). Haarpaintner *et al.* (2001b) report denser brine-enriched shelf waters formed during milder winters, due to a shallower position of the polynya on the shelf. The topography and the tidal currents also play an important role in determining the physical characteristics of the brine-enriched shelf waters by promoting the mixing of watermasses and the decrease of the density of the brine enriched shelf waters (Haarpaintner *et al.* 2001a, c).

Sediment sampling

During the STeP (Storfjorden Polynya Multidisciplinary Study) cruise on board the RV 'L'Atalante' (IFREMER) in July 2016, we sampled interface cores (9.6-cm internal diameter, 10-cm length) with a multi-corer at seven stations across an inner–outer fjord transect (Fig. 1). Three stations were sampled in the inner fjord (at ~110 m depth), two in the two central deep basins (at ~180 m), one over the sill (at ~160 m), and one in the Storfjorden Trough (at ~320 m; hereinafter called the outer fjord). All details related to the sampling stations are given in Table 1. At each station, except for MC3,

Table 1. Sampling date, coordinates, and sampling water depth of the seven stations sampled during the STeP mission.

Sampling date	Station	Latitude (N)	Longitude (E)	Depth (m)
13th July 2016	MC1	78°15.0′	19°30.0′	108.0
14th July 2016	MC2	77°50.0′	18°48.0′	117.0
14th July 2016	MC3	77°58.6′	20°14.6′	99.0
15th July 2016	MC4	77°29.2′	19°10.6′	191.5
17th July 2016	MC5	77°13.2′	19°17.9′	171.0
18th July 2016	MC6	76°53.9′	19°30.3′	157.0
19th July 2016	MC7	76°00.9′	17°03.4′	321.0

two cores were retrieved, one for foraminiferal analyses and one for age models.

Sedimentation rates

At each station (except for MC3), cores were sliced on board, collecting five sediment layers (0–0.5, 0.5–1, 1–2, 2–5 and 5–10 cm), then stored at −20 °C. In the laboratory, sediment samples were lyophilized to perform gamma spectrometry measurements to determine the apparent sedimentation rate by the $^{210}Pb_{xs}$ method (Appleby & Oldfield 1978). The ^{210}Pb dating was conducted using a gamma spectrometer Mirion Canberra HPGe GX4520 coaxial photon detector at Subatech Laboratory Nantes. The homogenized samples were weighed and sealed in a defined geometry for at least 3 weeks to ensure ^{222}Rn–^{226}Ra–^{214}Pb equilibration. The sedimentation rate was calculated by determining the excess or unsupported activity of ^{210}Pb ($^{210}Pb_{xs}$) using the constant flux-constant sedimentation (CF-CS) model (Sanchez-Cabeza & Ruiz-Fernández 2012). The $^{210}Pb_{xs}$, incorporated rapidly into the sediment from atmospheric fall-out and water column scavenging, was calculated as the difference between the total measured activity of ^{210}Pb (supported + excess) at 46.54 keV and of ^{214}Pb at 351.93 keV.

The depth of the surface mixed layer was established on the basis of homogenous $^{210}Pb_{ex}$ activity. This homogeneity is the result of physical (resuspension/deposition) and/or biological disturbance (e.g. Schmidt *et al.* 2005). The surface mixed layer does not correspond exactly to the bioturbation depth, because bioturbation can still occur in the deeper incomplete mixing layers (Tomašových *et al.* 2019). However, below the surface mixed layer, bioturbation coefficients are generally much lower (10–20%; Silverberg *et al.* 1986), up to several orders of magnitude (Muñoz *et al.* 2004) and thus, their influence on taphonomic processes is reduced or negligible. The TAZ, defined as the zone of the sediment included between the surface and the bottom of the bioturbated area (Berkeley *et al.* 2007), was therefore considered as corresponding to the surface mixed layer of the sediment (i.e. $^{210}Pb_{ex}$ activity).

Foraminiferal analyses

Interface sediment cores dedicated to foraminiferal analyses were sliced every 0.5 cm down to 2-cm depth, then 1 cm down to 6-cm depth and 2 cm down to 10-cm depth. Each sediment sample was stained with 2 g L^{-1} Rose Bengal in ethanol to distinguish living and dead specimens. Once in the laboratory, the samples were washed using 63, 125 and 150 μm meshed sieves. The living specimens were hand-picked in water and analysed together with geochemical and sedimentological parameters in the top 5 cm of the sediment by Fossile *et al.* (2020). Plates with SEM pictures of the most abundant foraminiferal species can be found in the supplement section of Fossile *et al.* (2020). For dead (i.e. above the TAZ) and fossil (i.e. below the TAZ) faunal analyses, the residual samples were dried at 50 °C. When the densities were high, the dry residues were split using an OTTO microsplitter. A minimum of 300 individuals were picked from a single split and the counts were then standardized to the total sample. These analyses were performed on the >150 μm fraction of the dead assemblage (0–1 cm) and fossil assemblages (3–4 and 6–8 cm sediment layers). The size fraction to consider was chosen based on the observations of Fossile *et al.* (2020), who noted that the large size fraction (>150 μm) gives similar ecological information to the small size assemblages (63–150 μm) in the study area. Foraminiferal densities for dead (0–1 cm) and fossil (3–4, 6–8 cm) faunas, and the list of the species can be found in the Supporting Information (Tables S1–S3).

Foraminiferal densities in the 3–4 and 6–8 cm sediment layers are supposed to represent the fossil or preserved fraction of fauna integrating (i) foraminifera living at the surface sediment at the time when the layer was located at the water–sediment interface and (ii) the infaunal foraminifera that lived in this layer after its burial. These two sediment layers are supposed to lie below the TAZ, where bioturbation can have a strong influence on sediment reworking and early diagenesis (Berkeley *et al.* 2007, 2014). Therefore, they should contain early fossil assemblages having undergone the first steps of taphonomic processes. The two sediment layers were analysed to eventually detect significant differences that would have indicated strong diagenetic processes occurring below the TAZ. Fossil foraminifera from both layers were compared to living faunas (in the 0–1 and 0–5 cm sediment layers) and to the dead fauna from the topmost centimetre, to estimate taphonomic loss.

To compare faunas from sediment layers of different volumes and sampled at different depths in the core (i.e. with possible differences in the compaction state), we normalized and expressed foraminiferal absolute abundances as individuals per gram of dry sediment. As the foraminiferal samples were not weighed before sieving, we estimated the water content

of each layer from the analyses of twin cores sampled at each station for other sedimentological analyses. Wet and dry sediment layers of these cores were weighed, and the porosity calculated on the basis of the water content. The raw number of picked foraminifera being standardized for 50 cm^3 (wet sediment), the volume of water was subtracted from this volume, and the remaining was converted to massof sediment by multiplying by sediment density (a density of 2.6 g cm^{-3} was used as an average for clay-silt sediment particles, e.g. Blake 2008).

To quantitatively estimate the differences between living and fossil assemblages, the L/(L + F) ratio was calculated using the relative abundances of the major species (Jorissen & Wittling 1999). In the following formula $L_{0–5\ cm}/(L_{0–5\ cm} + F_{6–8\ cm})$, L indicates the relative abundance of each living species in the 0–5 cm sediment layer whereas F indicates the relative abundance of each fossil species from the 6–8 cm sediment layer. For each species, ratios between 0 and 0.5 indicate that the species is relatively more abundant in the fossil fauna, ratios between 0.5 and 1 indicate that it is more abundant in the living faunas, whereas a value of 0.5 means an equal representation.

The A/C ratio is calculated as the ratio of relative abundances of the agglutinated and calcareous (miliolids and hyaline) species. As the fossil layers are supposed to integrate the fauna living in all microhabitats (including infaunal) and in all seasons (fauna of the year) we compared the A/C ratio of the whole living assemblages (0–5 cm) and of the annual fauna (total = living + dead, 0–1 cm) with that of the fossil layer (6–8 cm) to detect possible changes due to taphonomy.

Results

Sediment accumulation rate and determination of the taphonomically active zone

The results for $^{210}Pb_{xs}$ are reported in Fig. 2. The surface mixed layer, where the sediment is distinctly bioturbated, can be identified through the unvaried ^{210}Pb activity values in the topmost centimetre of the cores. This depth is identified as the limit of the taphonomically active zone. The $^{210}Pb_{xs}$ values for the surface mixed layer (in red in Fig. 2) are excluded from the sediment accumulation rate (SAR) estimation. The SAR is particularly high inside the fjord (0.26±0.09 to 0.39±0.03 cm a^{-1} at stations MC2 to MC5) and lower at the outer MC7 station (0.13±0.06 cm a^{-1}). The precision of the SAR obtained for stations MC1 and MC6 is too low to be considered as reliable (error >2σ). The slope of the linear model for $^{210}Pb_{xs}$ measurements in core MC7 is strongly driven by the deepest point, which could be the result of irregular sedimentation at this station.

Taphonomic loss

Density. – The analysis of the total fauna (living + dead foraminifera) in the 0–1 cm layer (Fig. 3A) shows the same order of magnitude for total densities between stations, with MC6 (sill) and MC1 (inner fjord) showing the lowest densities (~20 and 40 ind. g^{-1}, respectively), and station MC7 (outer fjord) showing the highest density (85 ind. g^{-1}). However, while inside the fjord (MC1 to MC6) most of the superficial fauna is represented by living specimens (>80%), the high density at the outer fjord MC7 is largely represented by dead faunas (65%).

The comparison of total densities (living + dead, 0–1 cm) with those of fossil fauna at 3–4 cm (Fig. 3B) and 6–8 cm (Fig. 3C) shows generally lower densities for the stations located inside the fjord (MC1 to MC5). This is particularly striking for station MC3, where fossil faunas are nearly absent (2 ind. g^{-1}). At station MC6 this is true for the 3–4 cm layer (~10 ind. g^{-1}) but densities are slightly higher at 6–8 cm (~30 ind. g^{-1}). At station MC7, fossil faunas are denser (~120 ind. g^{-1}) than in the total assemblage of the topmost centimetre (~90 ind. g^{-1}). No major differences are observed between the 3–4 and 6–8 cm layers except for the three times lower densities observed at station MC6 at 3–4 cm depth.

Species composition. – In Fig. 4, the relative abundances of the 21 major species (>5% in at least one layer) are shown for the living assemblages of the first 5 cm of sediment, living and dead assemblages of the 0–1 cm layer, and the fossil faunas at 3–4 and at 6–8 cm.

In the inner fjord stations (MC1 to MC3), the living (0–1 and 0–5 cm) and the dead faunas (0–1 cm) are mainly represented by the same major species, *Elphidium clavatum* and *Nonionellina labradorica* (the latter is more abundant when subsurface layers are considered). In both the fossil assemblages of these inner fjord stations (at 3–4 and 6–8 cm depths), the same species dominate, with comparable proportions between the two sediment layers. Despite the very low densities observed for the MC3 fossil faunas (i.e. ~2 ind. g^{-1} at both 3–4 and 6–8 cm depth; Fig. 3B, C), the major species are still represented. *Cassidulina reniforme*, limited to the MC1 station, is represented at each considered depth. *Elphidium clavatum* at MC3 shows reduced percentages in the fossil faunas (both at 3–4 and 6–8 cm) compared to the living and dead assemblages (~40 vs. 80%, respectively). Conversely, *Ammotium cassis* is nearly absent in the living and dead faunas and reaches about 20% in the fossil assemblages. The calcareous *Buccella frigida* is nearly absent in the living faunas and its relative abundances increase in the dead and fossil assemblages (5–15%).

In the deep basins (MC4 and MC5) and sill (MC6) stations, living faunas and dead faunas of the topmost

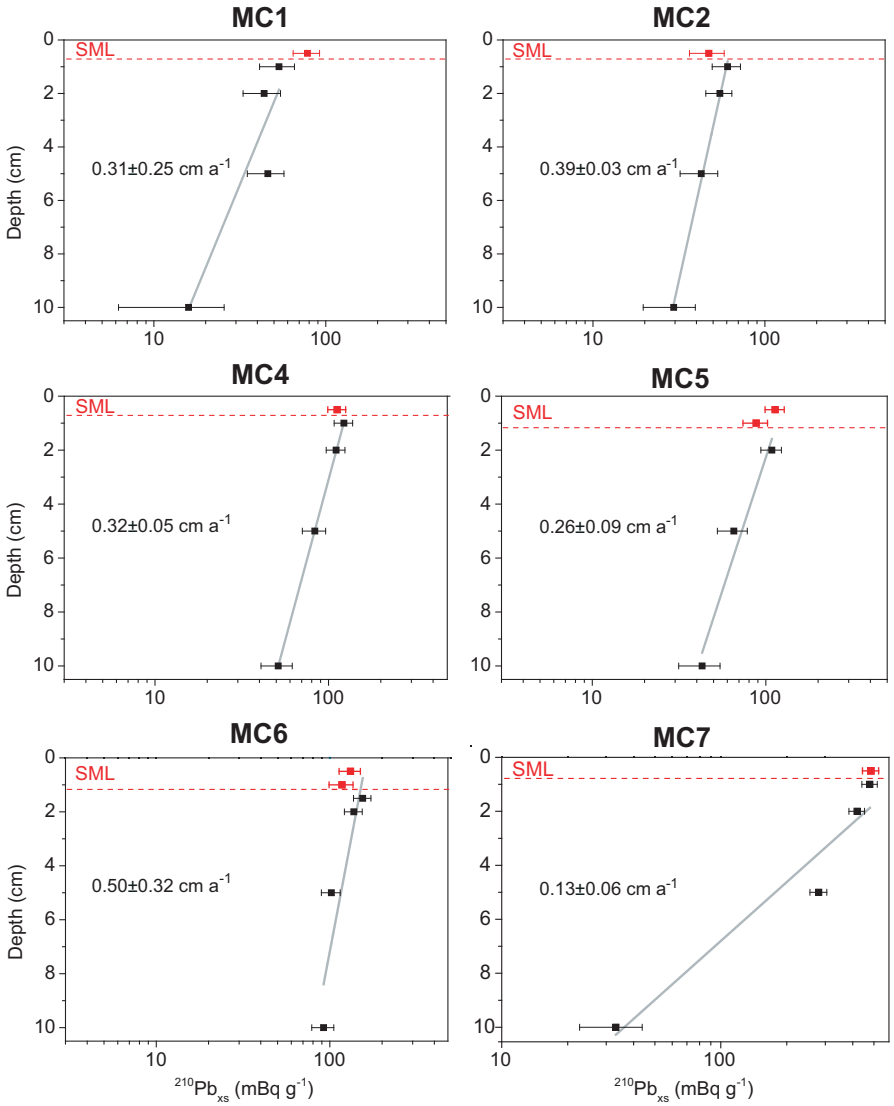

Fig. 2. $^{210}Pb_{xs}$ incorporation into sediment from the sediment surface down to 10-cm depth and the corresponding sediment accumulation rates expressed as cm a^{-1}. The dashed lines correspond to the limit of the surface mixed layer (SML), also identified as the TAZ. In red are reported the $^{210}Pb_{xs}$ points included in the SML.

centimetre are largely represented by *Reophax* spp. (30–50%), *Recurvoides turbinatus* (10–25%) and *Labrospira crassimargo* (5–15%). These agglutinated species are accompanied by 8–10% of *N. labradorica* in the living assemblages of the 0–5 cm sediment layers. At station MC6, a high proportion of *Adercotryma glomeratum* is also observed (10–30%). The proportions of *L. crassimargo* and *R. turbinatus* are comparable in both the 3–4 and 6–8 cm fossil assemblages, whereas *Reophax* spp. drastically decreases to reach 0–12%. *Adercotryma glomeratum* reaches only 5% in the deeper fossil faunas (6–8 cm). Some calcareous species become noticeable only in the fossil faunas, such as *Elphidium clavatum* (about 10–25%), *Elphidium bartletti* (about 5–13% in the 6–8 cm) and *C. reniforme* (10%) at MC4.

The living and dead assemblages at the outer fjord station MC7 show high proportions of *Reophax* spp. (15–35%), *Lagenammina difflugiformis* (10–25%) and *Melonis barleeanus* (~10%), accompanied by *N. labradorica* in the 0–5 cm (25%) and in the dead assemblages of the 0–1 cm layer (15%). In the fossil assemblages of both the 3–4 and 6–8 cm sediment layers, the agglutinated species are nearly absent, and the relative abundance of *M. barleeanus* remains the same while the proportion of *N. labradorica* decreases to 5–10%. Furthermore, some calcareous species are only present in the fossil assem-

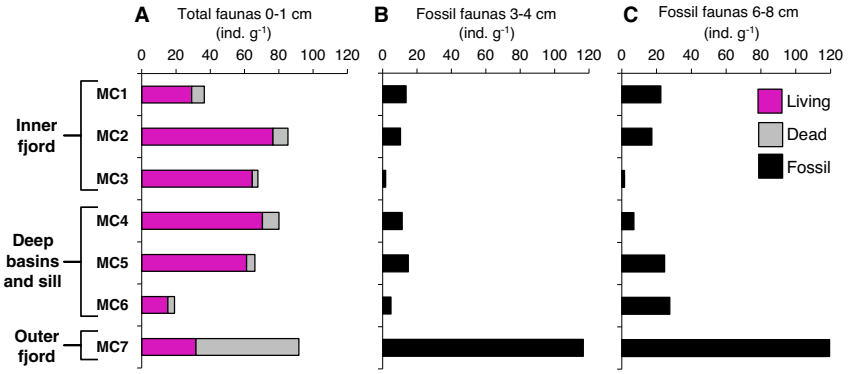

Fig. 3. Foraminiferal densities expressed in individuals per gram of dry sediment (ind. g^{-1}) considering the (A) total faunas (living + dead) in the 0–1 cm sediment layer, (B) the fossil faunas in the 3–4 cm and (C) 6–8 cm sediment layers.

blages (e.g. *Cribroelphidium subarcticum*, 10%) or in both dead and fossil assemblages (e.g. *E. clavatum*, 10–20%).

Living vs. fossil assemblages. – To quantitatively estimate the difference between the species composition of the living and fossil assemblages, the $L_{0–5\ cm}/(L_{0–5\ cm} + F_{6–8\ cm})$ ratio was calculated for 19 major species (Fig. 5). The $^{210}Pb_{xs}$-based estimation of sedimentation rates shows that both the 3–4 and 6–8 cm layers were below the TAZ. The differences in terms of species composition between the two layers are low at all stations. Since the older layer (6–8 cm) has undergone taphonomic processes for a longer period than the 3–4 cm layer, this is regarded as the best representative for the fossil assemblages and therefore presented in Fig. 5 for comparison. In the inner fjord, the ratio for the calcareous *Elphidium clavatum* is about 0.3 at MC1 and it increases to 0.5 and 0.6, respectively, at MC2 and MC3. *Nonionellina labradorica* shows a ratio from about 0.6–0.8 at MC1 and MC2 to about 0.4 at MC3. In the inner fjord, the only major agglutinated species is *Ammotium cassis* at MC3, which shows a ratio of 0.3.

In the deep basins (MC4 and MC5) and sill (MC6) stations all the calcareous species show ratios <0.5, except for *N. labradorica* at MC4 (0.6 ratio) and *Nonionella digitata* at MC5 (0.9 ratio). The agglutinated taxa *Reophax* spp., *Recurvoides turbinatus*, *A. cassis* generally have ratios of about 0.6 to 1 in these stations. The exceptions are *R. turbinatus* at MC4, showing a ratio of 0.4, and *Labrospira crassimargo* with 0.4–0.5 ratios at MC4 and MC5. Finally, a ratio of 0.8 is observed for *Adercotryma glomeratum* at the sill station MC6.

In the outer fjord, MC7, *Buccella frigida*, *Cassidulina teretis*, *Cibicidoides lobatulus*, *Cribroelphidium subarcticum* and *E. clavatum* have ratios <0.2. *Globobulimina auriculata* and *N. labradorica* show 0.8–1 ratios. Concerning the agglutinated taxa, *Reophax* spp. and *Lagenammina difflugiformis* have ratios of 0.9–1.

Agglutinated/calcareous (A/C) ratio

The A/C ratios were calculated from the relative abundances of species from the living faunas (0–5 cm; Fig. 6A; Fossile *et al.* 2020), the total faunas (living + dead in the 0–1 cm; Fig. 6B) and from the fossil faunas at 6–8 cm depth (Fig. 6C).

The A/C ratio at the inner fjord stations (MC1 to MC3) is <0.1 due to high relative abundances of calcareous species (i.e. 89–94%) in the living (0–5 cm; Fig. 6A), total (living + dead, 0–1 cm; Fig. 6B) and fossil (6–8 cm; Fig. 6C) faunas. The only noticeable difference is the slight increase in the ratio from 0.1 to 0.2 for the fossil assemblages at MC3.

In the deep basin and sill stations (MC4 to MC6) the A/C ratio varies between 1.9 and 3.4 in the living faunas (0–5 cm; Fig. 6A), and it increases up to 3.0–6.2 for the total faunas (living + dead, 0–1 cm; Fig. 6B). This is determined by high percentages of agglutinated species (i.e. 65–86%). In the fossil faunas (6–8 cm; Fig. 6C), the A/C ratio decreases to values of 0.3–0.5 (agglutinated species about 20–33%), but it is still two to three times higher than in the inner fjord stations.

In the outer fjord station MC7, the ratio is about 0.7–0.8 in the living (0–5 cm; Fig. 6A) and total faunas (living + dead; Fig 6B) due to the high proportion of calcareous species (about 60%). The ratio decreases to 0.03 in the fossil faunas (6–8 cm; Fig. 6C) due to a stronger dominance of calcareous species (95%).

Discussion

Ecological and taphonomic processes affecting foraminiferal standing stocks

Foraminiferal total fauna (dead + living) represents the integration of most of the specimens inhabiting a given place over a certain period. According to the estimated sedimentation rates, the total faunas of the 0–1 cm layer integrate approximately 2.5–4 years' period

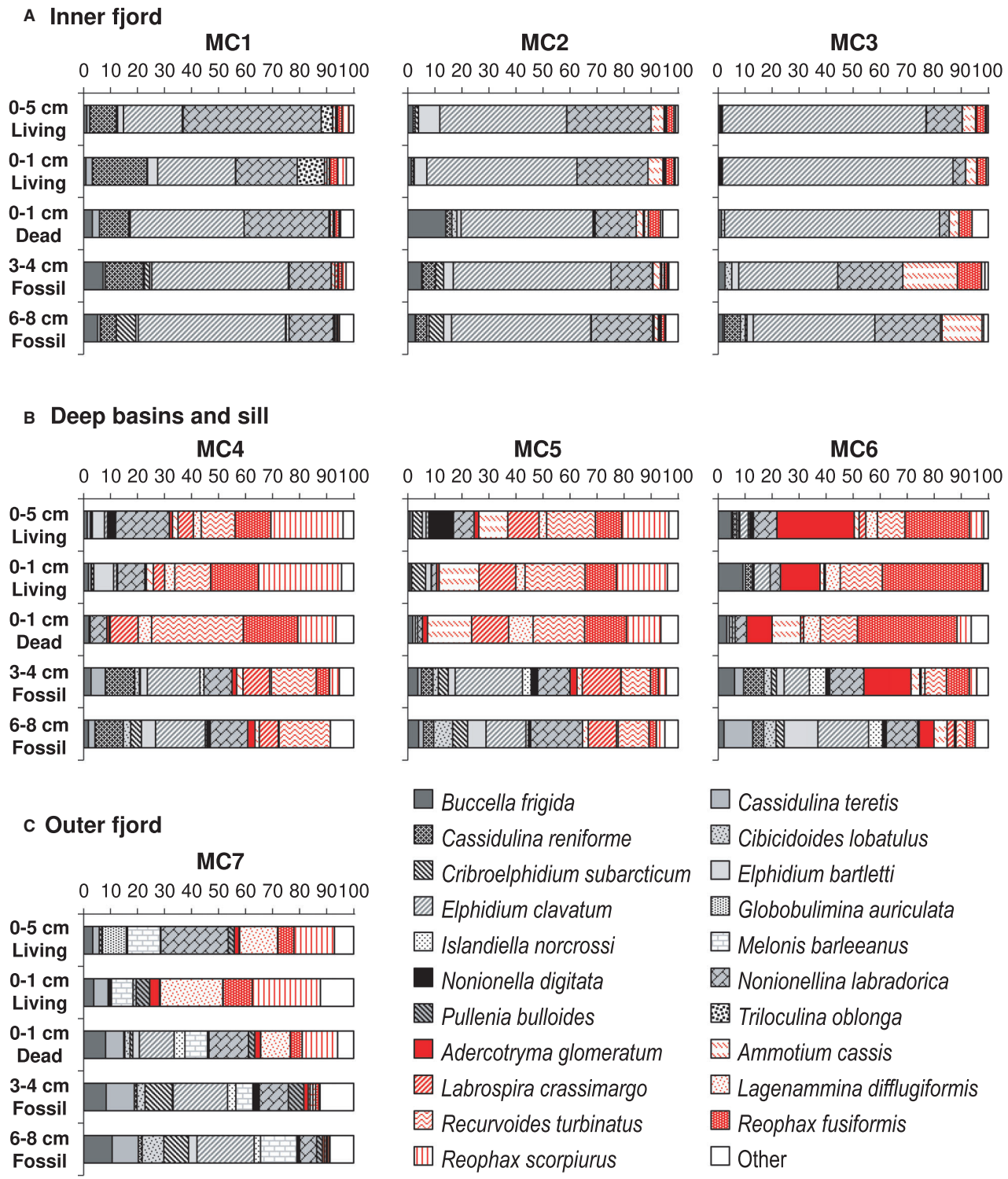

Fig. 4. Relative abundances of the 21 major species (>5% in at least one layer) considering the living faunas from the 0–5 and 0–1 cm sediment layers, the dead faunas from the 0–1 cm sediment layer and the fossil faunas from the 3–4 and 6–8 cm sediment layers for (A) the inner fjord, (B) the deep basins and sill and (C) the outer fjord. Red textures represent agglutinated species and grey ones the calcareous species. "Other" category includes both agglutinated and calcareous rare species.

(Fig. 2). The accumulation of dead faunas depends both on species production and taphonomic factors (e.g. Schönfeld *et al.* 2012). The comparison between living and dead faunas from the topmost centimetre of the sediments in Storfjorden (Fig. 3A) shows a major difference between the stations inside the fjord (MC1 to

MC6) and the outer fjord station (MC7). Inside the fjord, the dead assemblages of the top centimetre account for only 5–20% of the total fauna while in the outer station MC7, they represent about 65% of the total assemblage. This difference may be explained by a seasonal contrast in foraminiferal densities between summer (the sampling season) and other seasons, coupled to more intense early taphonomic processes inside than outside the fjord.

Indeed, the winter in the Arctic realm, including Storfjorden, is characterized by the scarcity of light and by water stratification (Howe *et al*. 2010; Berge *et al*. 2015a, b). This seasonal physical setting controls the timing and rate of primary productivity, and the associated organic fluxes to the sea floor, which largely increase during spring–summer. Increased density and diversity of meiofauna and macrofauna were observed in the Adventfjorden (Svalbard, Fig. 1), as a response to meltwater discharges and increased primary productivity during the warm season (Pawłowska *et al*. 2011). As benthic meiofaunal consumers, foraminifera may as well lower their production rate during winter to adapt to low organic matter fluxes (e.g. Pawłowska *et al*. 2011; Juul-Pedersen *et al*. 2015) and increase their abundances during the warm season. Such seasonal and interannual variability in living foraminiferal densities was reported recently from Kongsfjorden, another Svalbard fjord (Fig. 1), and was inferred to be a result of temporal variability in primary productivity (Jernas *et al*. 2018). In our case study, this would explain the high densities of living foraminifera (i.e. warm-seasonal faunas of the year, Fig. 3) compared to dead assemblages, inside the fjord (MC1 to MC6). The observed dead assemblages would mainly represent the rest of the living faunas of the previous warm seasons, after potentially high early taphonomic loss, rather than faunas of cold seasons. In accord with this hypothesis, the higher proportion of dead faunas at MC7 would be at least partially due to weaker seasonal contrast in foraminiferal densities, and potentially coupled to reduced taphonomy at this station. Indeed, inside the fjord, the production and cascading of corrosive brine-enriched shelf waters during winter–early spring enhance early taphonomic processes close to the sediment surface, leading to a partial or total dissolution of calcitic-shelled foraminifera as reported by Fossile *et al*. (2020). Additionally, higher fluxes of organic matter during the warm season, and its enhanced remineralization, can contribute to further lowering of the pH in the first layers of the sediment column (Fossile *et al*. 2020). As such, the resulting dissolution of calcitic shells may explain the low percentages of dead faunas in the fjord stations. Outside the fjord, the influence of brine-enriched shelf waters is episodic and only related to the seasonal outflow during their production period (Skogseth *et al*. 2005a).

In addition to these hypotheses, the difference in sedimentation rates may also be a reason for the observed contrasts among stations. Outside the fjord, the sedimentation rates are on average three times lower than inside. This, added to the reduced influence of brine-enriched shelf waters, promotes the accumulation of dead faunas at MC7 (see Fig. S1).

The difference in the preservation potential observed in the upper centimetre faunas between the stations inside and the one outside the fjord, is also observed in the fossil faunas from the 3–4 and 6–8 cm sediment layers (Fig. 3). Except for the sill station MC6, where standing stock fluctuations among layers are observed, the stations inside the fjord (MC1–MC5) generally show low preservation of fossils (Fig. 3), while an accumulation of specimens is visible outside the fjord (MC7). The higher variability observed at station MC6 highlights the possible influence of natural temporal variability of standing stocks on fossil assemblage accumulation. This could be due to biological reasons (increased reproduction rates at some periods) and/or to physical processes influencing accumulation, including transport over the sill during brine outflows (e.g. Nielsen & Rasmussen 2018).

The generally high similarity, in terms of standing stocks, between fossil faunas at 3–4 and 6–8 cm depths (Fig. 3) at all stations confirms that: (i) the maximum taphonomic loss occurs at the sediment surface (within the TAZ), (ii) both 3–4 and 6–8 cm sediment layers contain fossil faunas that went through the early taphonomic stages, and (iii) there is not a major taphonomic loss occurring between the 3–4 cm and 6–8 cm layers.

Species preservation in the fossil record

Species compositions of the living (0–1 and 0–5 cm), dead (0–1 cm) and fossil (3–4 and 6–8 cm) assemblages show different results for calcareous and agglutinated species in terms of preservation potential.

In the innermost fjord stations (MC1 to MC3), all the assemblages (i.e. living, dead and fossils) are largely dominated by the same calcareous species (*Elphidium clavatum*, *Cassidulina reniforme* and *Nonionellina labradorica*). This indicates a low temporal variability in this part of the fjord. The presence of these species in the living assemblages, which reflect summer conditions, may indicate their tolerance to the potentially stressful environmental conditions during the melting season (i.e. high freshwater and sediment inputs from glaciers) and their preference for and/or tolerance of high concentrations of (fresh) organic matter (e.g. Hald & Korsun 1997; Korsun & Hald 1998; Forwick *et al*. 2010; Fossile *et al*. 2020). The low variability observed between dead and fossil assemblages in the inner fjord (MC1 to MC3) suggests that the fossil faunas mostly reflect, in terms of species composition, the summer foraminiferal assemblages. The alternative hypothesis would be the dissolution of cold season faunas during the phases of intense brine production and cascading. Considering the living

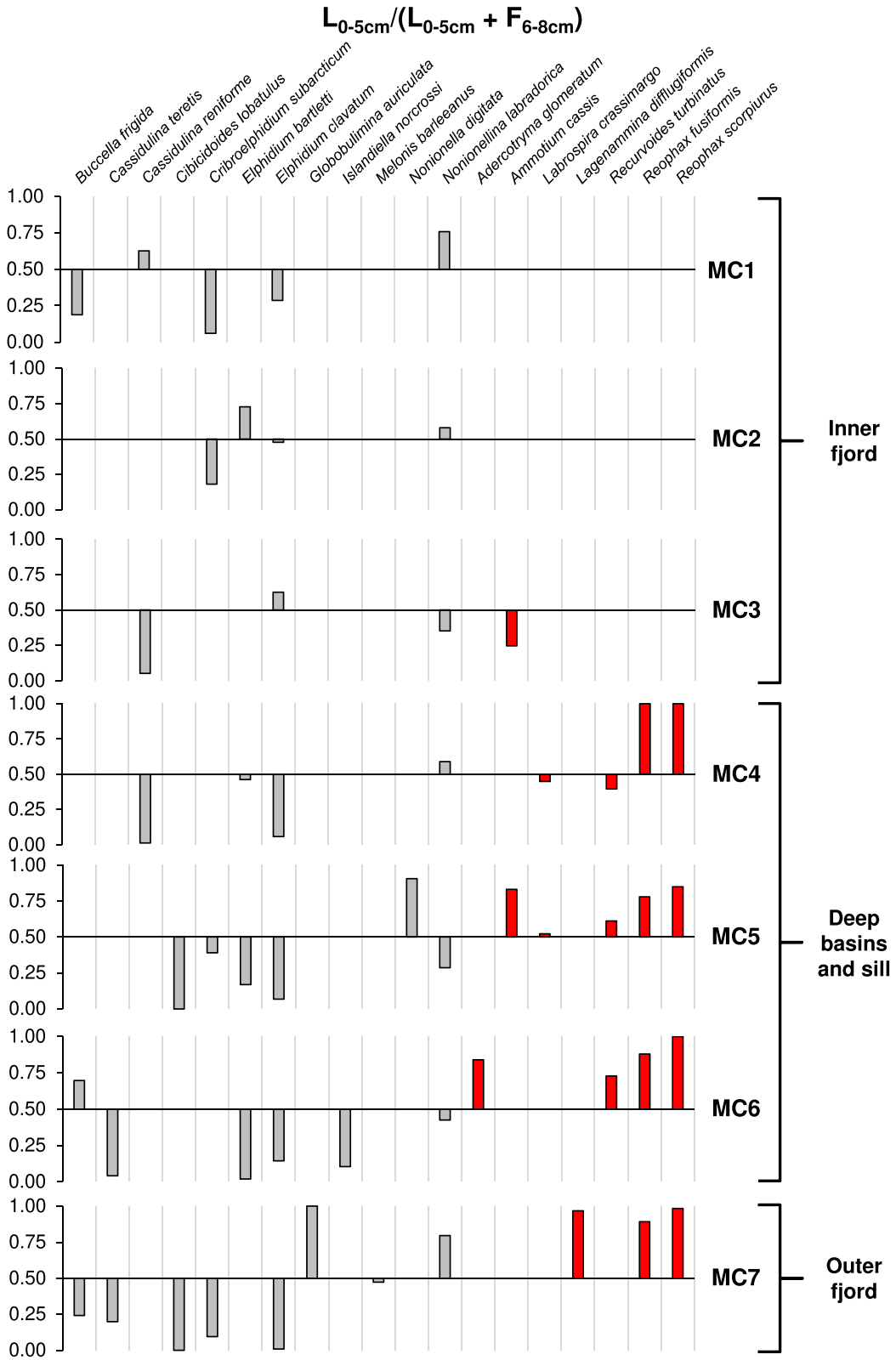

Fig. 5. Ratio between living faunas (from the 0–5 cm sediment layer) and the fossil faunas (from the 6–8 cm sediment layer) calculated as: $L_{0-5\ cm}/(L_{0-5\ cm} + F_{6-8\ cm})$. Ratios for calcareous species are reported in grey, ratio for agglutinated species in red. Ratio between 0.5 and 1 indicates a relatively higher representation of the present-day species in the living faunas, a ratio between 0 and 0.5 a higher representation of the species in the fossil faunas, whereas a value of 0.5 shows an equal representation.

assemblages, the low proportion of *E. clavatum* in favour of *N. labradorica* in the 0–5 cm layer compared to the sediment surface (0–1 cm) reinforces the need of including infaunal microhabitats in the comparisons of living and fossil faunas, to avoid underestimating infaunal species.

In our samples, there is only one calcareous species, *Buccella frigida*, which is abundant only in the dead/fossil assemblages and nearly absent in the living fauna. This species has been previously reported from glacier-proximal areas of Arctic fjords (e.g. Korsun & Hald 1998; Jernas *et al*. 2013) and suggested by Szymańska *et al*. (2017) as an indicator of sea-ice formation during winter. Its presence in the dead faunas may suggest its occurrence only during the winter season. This corroborates that winter faunas are not completely impacted by taphonomy and that the dead and fossil assemblages reflect most likely a higher level of foraminiferal production in summer. Another possibility could be that *B. frigida* resists dissolution better than other winter species, which would therefore not be preserved in dead and fossil faunas. However, species relative abundances are comparable in the fossil faunas, suggesting no species-specific taphonomic loss. The only exception is *E. clavatum*, which seems to suffer high taphonomic loss in terms of relative abundances (Fig. 4) but it is still well represented in the fossil assemblages.

In the deep basins (MC4 and MC5) and sill (MC6) stations, the living faunas are dominated by agglutinated species, including fragile organic-cemented agglutinated taxa such as *Reophax* spp. (e.g. Schröder 1988). The dead faunas at these stations (MC4–MC6) are similar to the living assemblages, suggesting that the diagenesis of agglutinated tests does not occur rapidly after their death, despite the persistence of brine-enriched shelf waters as previously reported by Fossile *et al*. (2020). This is in accord with Rasmussen & Thomsen (2015) who reported the presence of *Reophax* spp. in Holocene archives from central Storfjorden and suggested that the high sedimentation rates of the fjord were responsible for the exceptional preservation of these species. In our samples, however, the fossil faunas show a clear shift towards the dominance of calcareous species, while the agglutinated taxa, after the loss of fragile species, are mostly represented by the more robust agglutinated species *Adercotryma glomeratum*, *Ammotium cassis*, *Recurvoides turbinatus* and *Labrospira crassimargo* (Figs 4, 5), which may have a better preservation potential (e.g. Rasmussen & Thomsen 2015). As such, the higher proportion of calcareous species in the fossil faunas at these stations would mainly be the consequence of selective taphonomic loss of some agglutinated species that are dominant in the living fraction (e.g. *Reophax* spp.).

Differently from the inner fjord, where the dominant calcareous species do not change among layers, in the deep basins and sill stations, some major changes in calcareous species composition are observed. For instance, *E. clavatum* is nearly absent in the living faunas of the deep basins and, when present, it shows high degrees of dissolution (Fossile *et al*. 2020). Its higher relative density in the living faunas of the sill station MC6 could be related to the only intermittent influence of brine-enriched shelf waters over the sill. The quite high relative abundance of *E. clavatum* in the fossil faunas of the stations MC4 to MC6 therefore, could be indicate either past conditions with different environmental characteristics in this area of the fjord (i.e. more similar to inner fjord, lower influence of brine-enriched shelf waters) or possible transportation from the inner fjord with BSW cascading or near-bottom currents, followed by a rapid burial. As, according to the literature, deep

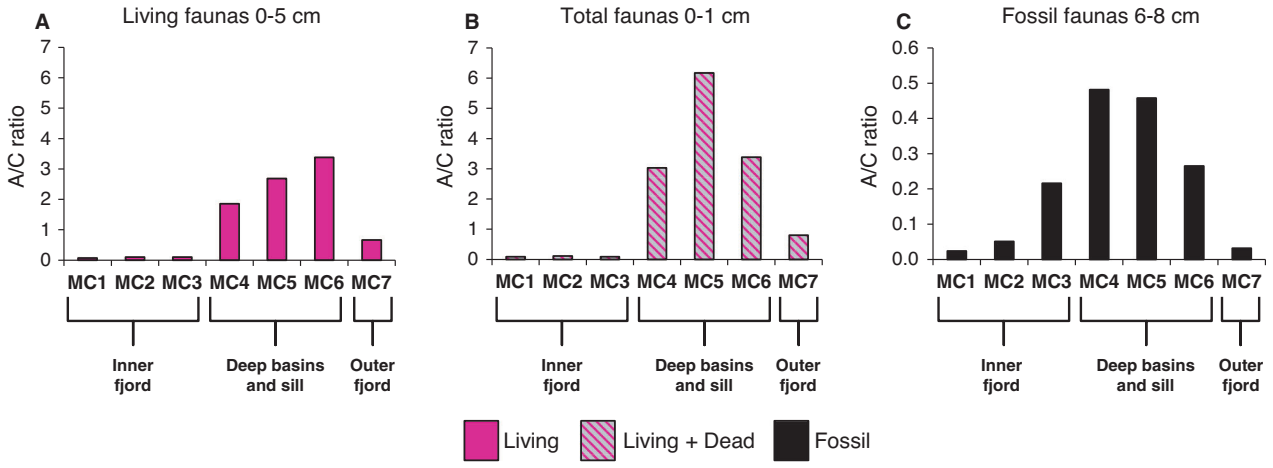

Fig. 6. Agglutinated/calcareous (A/C) ratio calculated for (A) living faunas from the 0–5 cm sediment layer, (B) total faunas (living + dead) from the 0–1 cm sediment layer and (C) fossil faunas from the 6–8 cm sediment layer. Note that the ratio scale is different for the fossil faunas compared with that of the others.

basins are characterized by constant conditions under year-round persisting brine-enriched shelf waters (Skogseth *et al*. 2005a), transport seems the most reliable hypothesis to retain. Moreover, the increased presence of *E. clavatum* in the fossil faunas is coeval with increased abundances of *Cibicidoides lobatulus*. The latter species has been previously reported from glacier-proximal stations in Storfjorden (e.g. Mackensen & Schmiedl 2016) and is often associated with coarse sediments and high-energy environments in the outer or threshold area of various Arctic fjords (e.g. Hald & Korsun 1997). Its presence in the fossil faunas would be is in accordance with the hypothesis of intermittent transport by near-bottom currents or brine-enriched shelf waters cascading formulated for *E. clavatum*.

Among the calcareous species found in the deep basins (MC4 and MC5) and sill (MC6) stations, *N. labradorica* is highly abundant in all the assemblages and does not show high degrees of dissolution in the living assemblages directly under the influence of corrosive brine-enriched shelf waters (Fossile *et al*. 2020). Although the reason for such a resistance to dissolution is intriguing, this seems to be the only possible explanation of its high preservation potential in the fossil record (Figs 4, 5). The resistance could be related to a high level of robustness of the shell or to physiological adaptative patterns. Indeed, the pH values in the first millimetres or centimetre of the sediment are typically lower than at the water–sediment interface, due to aerobic respiration of organic matter. As a shallow to deep infaunal species (e.g. Fontanier *et al*. 2014), *N. labradorica* could be adapted to calcify under low pH conditions, and as such, this might be an advantage for preservation in environments affected by corrosive brine-enriched shelf waters.

Finally, we highlight that the outer fjord station MC7 shows very different assemblages when comparing living and fossil faunas. Living faunas are composed of typical Atlantic species, such as *Melonis barleeanus*, *Cassidulina teretis* and *Globobulimina auriculata* (e.g. Jennings *et al*. 2004; Knudsen *et al*. 2012; Jernas *et al*. 2018). While *M. barleeanus* and *C. teretis* are still well represented in the dead and fossil assemblages, *G. auriculata* is completely absent in the fossil record. The latter species has a very thin and delicate calcareous test, with consequent lower fossilizing potential, suggesting a possible selective taphonomy against this species. Fossil faunas show an interesting mix of Atlantic and Arctic species (i.e. *B. frigida*, *E. clavatum*, *N. labradorica*). This station, located at about 300 m depth in the Storfjordrenna, about 50 km from the southern coast of Spitsbergen, is possibly influenced both by Atlantic waters (during summer, Fig. 1) and brine-enriched shelf water overflows from Storfjorden during winter–early spring (i.e. the period of intensive sea-ice formation). Accordingly, the presence of both Atlantic and Arctic species is representative of the seasonal variability in the assemblage composition at the outer fjord.

The A/C ratio as a proxy for historical reconstructions of brine persistence

The comparison between recent (living and dead) and fossil assemblages in terms of shell composition shows that the effects of brine persistence in the bottom waters (as observed by Fossile *et al*. 2020) are still visible after the first phases of taphonomic processes. In fact, despite the considerable loss of foraminifera (e.g. both at 3–4 and 6–8 cm depth, Fig. 3), and the selective disappearance of delicate agglutinated taxa (mainly *Reophax* and *Lagenammina* spp.) or fragile calcareous species (e.g. *G. auriculata*), the A/C ratios still reflect the ratios calculated for the living faunas.

In absolute terms, A/C ratios decrease by one order of magnitude when comparing the 0–1 cm total (living and dead) faunas and the 6–8 cm fossil faunas. This is possibly due to the selective loss of agglutinated species as a result of taphonomic processes. This difference is smoothed when comparing the 0–5 cm living faunas to the fossil faunas (6–8 cm) because of the presence of calcareous species in the infaunal microhabitat (e.g. *Nonionellina labradorica*). This result underlines that the lower A/C ratio of the fossil faunas is not exclusively related to the preservation potential of agglutinated species but also to the fact that fossil assemblages integrate species from potentially different microhabitats.

Nevertheless, the loss of A/C signal between the recent faunas (total from 0–1 cm and living from 0–5 cm) and the fossil faunas (6–8 cm) does not invalidate the use of this ratio as a proxy for brine persistence. The A/C ratio, calculated on fossil faunas, in the deep basin is two to three times higher than in the inner fjord (Fig. 6). This confirms that the relative difference between the inner fjord stations (MC1–MC3), not impacted by persistent brines, and the deep basin and sill stations (MC4–MC6), influenced by long-term presence of brine-enriched shelf waters at the sea floor, is still clearly expressed.

Accordingly, our findings suggest that the A/C ratio can be used in historical sedimentary archives to determine the presence or absence of persistent brine-enriched shelf waters at the sea floor as an indirect proxy for thin first-year sea-ice production in coastal polynyas. The added value of the A/C ratio as a proxy for sea-ice production is its applicability in Arctic coastal settings where the common proxies for sea-ice reconstruction in open marine areas cannot be used (e.g. IP_{25}, Ribeiro *et al*. 2017; Limoges *et al*. 2018). Although our findings validate the use of the A/C proxy, we recommend its association with other proxies to obtain a more robust overview of historical sea-ice dynamics. For example, Ribeiro *et al*. (2017) performed a calibration of possible useful proxies in some fjords of Greenland and suggested that organic compounds, biogenic silica and a sea-ice-associated biomarker (i.e. HBI III) are reliable indicators of marine influence and sea-ice edge position in the fjord

system. The complementary application of the A/C ratio would allow the identification of events (or their absence) of first-year sea-ice production in the recent past (i.e. hundreds of years) in Arctic coastal/fjord settings.

Conclusions

The seasonal formation of sea ice and the consequent production of brine-enriched shelf waters undeniably impact the benthic environments in Storfjorden, as shown by foraminiferal assemblages, with clear spatial differences linked to the fjord topography. The persistence of corrosive brines at the sea floor is a major driving factor for foraminiferal distribution, leading to a relative increase of agglutinated species vs. calcareous species more sensitive to dissolution in the living assemblages. The present study validates the applicability of the agglutinated/calcareous (A/C) ratio as a proxy to reconstruct historical brine production and brine-enriched shelf water persistence at the sea floor, and indirectly, for a semi-quantitative estimation of the thin first-year sea-ice formation in the fjord. The *conditio sine qua non* for this validation was the preservation in the fossil records below the TAZ of the signal observed in living and recently dead faunas. Despite a high taphonomic loss in superficial sediment of Storfjorden in terms of standing stocks, the fossil faunas allow clear detection of the increased proportion of agglutinated species in the area persistently influenced by brine-enriched shelf waters (deep basins) compared to the one only influenced episodically (inner fjord). In Storfjorden and similar fjords characterized by the presence of deep basins delimited by a sill, analyses of cores sampled at or outside the sill would allow the persistence of brine-enriched shelf waters to be linked to intense overflow and therefore to the intense (or not) production of thin first-year sea ice. The possibility to reconstruct sea-ice dynamics in polar fjords on a historical time scale is crucial to confirm short time scale tendencies observed by satellite images on present-day ice cover and make more reliable predictions for the future.

Acknowledgements. – The research was funded by the ABBA (Observatoire des Sciences de l'Univers de Nantes Atlantique), Bi-SMART (University of Angers) and TANDEM (Région Pays de la Loire) projects. This research is part of the Ph.D. thesis of Eleonora Fossile, which is co-funded by French National Program MOPGA (Make Our Planet Great Again) and the University of Angers. We thank the captain and crew of RV 'L'Atalante', which was chartered by IFREMER (French Research Institute for Exploitation of the Sea); Frédéric Vivier (co-chief of the cruise); and all participants who contributed to the success of to the STeP cruise. We thank Bruno Bombled for his technical assistance during the cruise. We fully acknowledge the efficient technical help provided by Arbia Jouini and we thank Bruno Lansard and Caterina Morigi for the useful discussions about this research. We thank Karen L. Knudsen and one anonymous reviewer for their helpful comments, which helped to improve this manuscript.

Author contributions. – MPN and EF contributed equally to this work and are both first authors. EF: conceptualization, data curation, formal analysis, investigation, methodology, validation, visualization, writing – original draft, writing – review and editing. MPN: conceptualization, funding acquisition, investigation, resources, data curation, formal analysis, supervision, validation, writing original draft, writing – review and editing. OP: formal analysis, writing – review and editing. The authors declare no conflict of interest.

Data availability statement. – Foraminiferal densities for the living faunas (0–5 cm) are available from the following link: https://doi.org/10.1594/PANGAEA.907687 (Fossile *et al*. 2019).

References

Anderson, L. G., Falck, E., Jones, E. P., Jutterström, S. & Swift, J. H. 2004: Enhanced uptake of atmospheric CO_2 during freezing of seawater: A field study in Storfjorden, Svalbard. *Journal of Geophysical Research 109*, C06004, https://doi.org/10.1029/2003JC002120.

Appleby, P. G. & Oldfield, F. 1978: The calculation of lead-210 dates assuming a constant rate of supply of unsupported ^{210}Pb to the sediment. *Catena 5*, 1–8.

Belt, S. T. 2018: Source-specific biomarkers as proxies for Arctic and Antarctic sea ice. *Organic Geochemistry 125*, 277–298.

Belt, S. T. 2019: What do IP_{25} and related biomarkers really reveal about sea ice change? *Quaternary Science Reviews 204*, 216–219.

Belt, S. T. & Müller, J. 2013: The Arctic sea ice biomarker IP_{25}: a review of current understanding, recommendations for future research and applications in palaeo sea ice reconstructions. *Quaternary Science Reviews 79*, 9–25.

Belt, S. T., Massé, G., Rowland, S. J., Poulin, M., Michel, C. & LeBlanc, B. 2007: A novel chemical fossil of palaeo sea ice: IP_{25}. *Organic Geochemistry 38*, 16–27.

Bender, H. 1995: Test structure and classification in agglutinated foraminifera. *In* Kaminski, M. A., Geroch, S. & Gasiński, M. A. (eds.): *Proceedings of the Fourth International Workshop on Agglutinating Foraminifera 3*, 27–70. Grzybowski Foundation Special Publication, Kraków.

Berge, J. and 34 others 2015a: Unexpected levels of biological activity during the polar night offer new perspectives on a warming arctic. *Current Biology 25*, 2555–2561.

Berge, J., Renaud, P. E., Darnis, G., Cottier, F., Last, K., Gabrielsen, T. M., Johnsen, G., Seuthe, L., Weslawski, J. M., Leu, E., Moline, M., Nahrgang, J., Søreide, J. E., Varpe, Ø., Lønne, O. J., Daase, M. & Falk-Petersen, S. 2015b: In the dark: a review of ecosystem processes during the Arctic polar night. *Progress in Oceanography 139*, 258–271.

Berkeley, A., Perry, C. T., Smithers, S. G. & Hoon, S. 2014: Towards a formal description of foraminiferal assemblage formation in shallow-water environments: qualitative and quantitative concepts. *Marine Micropaleontology 112*, 27–38.

Berkeley, A., Perry, C. T., Smithers, S. G., Horton, B. P. & Taylor, K. G. 2007: A review of the ecological and taphonomic controls on foraminiferal assemblage development in intertidal environments. *Earth-Science Reviews 83*, 205–230.

Bizon, G. & Bizon, J. J. 1984: Méthode d'études et mode de prélèvement des sédiments d'ECOMED. *In* Bizon, J. J. & Burollet, P. F. (eds.): *Ecologie des microorganismes en Méditerranée occidentale "ECOMED"*, 81–83. Association Française des Techniciens du Pétrole, Paris.

Blake, G. R. 2008: Particle density. *In* Chesworth, W. (ed.): *Encyclopedia of Soil Science*, 504–505. Springer, Netherlands.

Davies, D., Powell, E. & Stanton, R. 1989: Relative rates of shell dissolution and net sediment accumulation - a commentary: can shell beds form by the gradual accumulation of biogenic debris on the sea floor? *Lethaia 22*, 207–212.

Fer, I., Skogseth, R., Haugan, P. M. & Jaccard, P. 2003: Observations of Storfjorden overflow. *Deep-Sea Research Part I: Oceanographic Research Papers 50*, 1283–1303.

Fontanier, C., Duros, P., Toyofuku, T., Oguri, K., Koho, K. A., Buscail, R., Grémare, A., Radakovitch, O., Deflandre, B., De Nooijer, L. J., Bichon, S., Goubet, S., Ivanovsky, A., Chabaud, G., Menniti, C.,

Reichart, G. J. & Kitazato, H. 2014: Living (stained) deep-sea foraminifera off Hachinohe (NE Japan, western Pacific): environmental interplay in oxygen-depleted ecosystems. *Journal of Foraminiferal Research 44*, 281–299.

Forwick, M., Vorren, T. O., Hald, M., Korsun, S., Roh, Y., Vogt, C. & Yoo, K.-C. 2010: Spatial and temporal influence of glaciers and rivers on the sedimentary environment in Sassenfjorden and Tempelfjorden, Spitsbergen. *Geological Society, London, Special Publications 344*, 163–193.

Fossile, E., Nardelli, M. P., Jouini, A., Lansard, B., Pusceddu, A., Moccia, D., Michel, E., Péron, O., Howa, H. & Mojtahid, M. 2020: Benthic foraminifera as tracers of brine production in Storfjorden "sea ice factory". *Biogeosciences 17*, 1933–1953.

Fossile, E., Nardelli, M. P. & Mojtahid, M. 2019: STEP2016 living foraminifera in surface sediments of a N-S transect in Storfjorden. *PANGAEA*, https://doi.org/10.1594/PANGAEA.907687.

Haarpaintner, J., Gascard, J. & Haugan, P. M. 2001a: Ice production and brine formation in Storfjorden, Svalbard. *Journal of Geophysical Research: Oceans 106*(C7), 14001–14013.

Haarpaintner, J., Haugan, P. M. & Gascard, J. C. 2001b: Interannual variability of Storfjorden (Svalbard) ice cover and ice production observed by ERS-2 SAR. *Annals of Glaciology 33*, 430–436.

Haarpaintner, J., O'Downer, J., Gascard, J. C., Haugan, P. M., Schauer, U. & Øterhus, S. 2001c: Seasonal transformation of water masses, circulation and brine formation observed in Storfjorden, Svalbard. *Annals of Glaciology 33*, 437–443.

Hald, M. & Korsun, S. 1997: Distribution of modern benthic foraminifera from fjords of Svalbard, European Arctic. *The Journal of Foraminiferal Research 27*, 101–122.

Howe, J. A., Austin, W. E. N., Forwick, M., Paetzel, M., Harland, R. E. X. & Cage, A. G. 2010: Fjord systems and archives: a review. *Fjord Systems and Archives 344*, 5–15.

Jennings, A. E., Weiner, N. J., Helgadottir, G. & Andrews, J. T. 2004: Modern foraminiferal faunas of the southwestern to northern Iceland shelf: oceanographic and environmental controls. *The Journal of Foraminiferal Research 34*, 180–207.

Jernas, P., Klitgaard Kristensen, D., Husum, K., Wilson, L. & Koç, N. 2013: Palaeoenvironmental changes of the last two millennia on the western and northern Svalbard shelf. *Boreas 42*, 236–255.

Jernas, P., Klitgaard-Kristensen, D., Husum, K., Koç, N., Tverberg, V., Loubere, P., Prins, M., Dijkstra, N. & Gluchowska, M. 2018: Annual changes in Arctic fjord environment and modern benthic foraminiferal fauna: evidence from Kongsfjorden, Svalbard. *Global and Planetary Change 163*, 119–140.

Jorissen, F. J. & Wittling, I. 1999: Ecological evidence from live-dead comparisons of benthic foraminiferal faunas off Cape Blanc (Northwest Africa). *Palaeogeography, Palaeoclimatology, Palaeoecology 149*, 151–170.

Juul-Pedersen, T., Arendt, K. E., Mortensen, J., Blicher, M. E., Søgaard, D. H. & Rysgaard, S. 2015: Seasonal and interannual phytoplankton production in a sub-Arctic tidewater outlet glacier fjord, SW Greenland. *Marine Ecology Progress Series 524*, 27–38.

Knudsen, K. L., Eiríksson, J. & Bartels-Jónsdóttir, H. B. 2012: Oceanographic changes through the last millennium off North Iceland: temperature and salinity reconstructions based on foraminifera and stable isotopes. *Marine Micropaleontology 84–85*, 54–73.

Korsun, S. & Hald, M. 1998: Modern benthic foraminifera off Novaya Zemlya tidewater glaciers, Russian Arctic. *Arctic and Alpine Research 30*, 61–77.

Limoges, A., Massé, G., Weckström, K., Poulin, M., Ellegaard, M., Heikkilä, M., Geilfus, N. X., Sejr, M. K., Rysgaard, S. & Ribeiro, S. 2018: Spring succession and vertical export of diatoms and IP_{25} in a seasonally ice-covered high Arctic fjord. *Frontiers in Earth Science 6*, 1–15.

Loeng, H. 1991: Features of the physical oceanographic conditions of the Barents Sea. *Polar Research 10*, 5–18.

Mackensen, A. & Schmiedl, G. 2016: Brine formation recorded by stable isotopes of recent benthic foraminifera in Storfjorden, Svalbard: palaeoceanographical implications. *Boreas 45*, 552–566.

Meredith, M., Sommerkorn, M., Cassotta, S., Derksen, C., Ekaykin, A., Hollowed, A., Kofinas, G., Mackintosh, A., Melbourne-Thomas, J., Muelbert, M. M. C., Ottersen, G., Pritchard, H. & Schuur, E. A. G. 2019: Polar Regions. *In* Pörtner, H.-O., Roberts, D. C., Masson-Delmotte, V., Zhai, P., Tignor, M., Poloczanska, E., Mintenbeck, K., Alegría, A., Nicolai, M., Okem, A., Petzold, J., Rama, B. & Weyer, N. M. (eds.): *IPCC Special Report on the Ocean and Cryosphere in a Changing Climate*, 203–320. Cambridge University Press, Cambridge, UK and New York, NY, USA. https://doi.org/10.1017/9781009157964.005.

Müller, J., Massé, G., Stein, R. & Belt, S. T. 2009: Variability of sea-ice conditions in the Fram Strait over the past 30,000 years. *Nature Geoscience 2*, 772–776.

Müller, J., Wagner, A., Fahl, K., Stein, R., Prange, M. & Lohmann, G. 2011: Towards quantitative sea ice reconstructions in the northern North Atlantic: a combined biomarker and numerical modelling approach. *Earth and Planetary Science Letters 306*, 137–148.

Muñoz, P., Lange, C. B., Gutiérrez, D., Hebbeln, D., Salamanca, M. A., Dezileau, L., Reyss, J. L. & Benninger, L. K. 2004: Recent sedimentation and mass accumulation rates based on ^{210}Pb along the Peru-Chile continental margin. *Deep-Sea Research Part II: Topical Studies in Oceanography 51*, 2523–2541.

Nielsen, T. & Rasmussen, T. L. 2018: Reconstruction of ice sheet retreat after the Last Glacial maximum in Storfjorden, southern Svalbard. *Marine Geology 402*, 228–243.

Ohshima, K. I., Nihashi, S. & Iwamoto, K. 2016: Global view of sea-ice production in polynyas and its linkage to dense/bottom water formation. *Geoscience Letters 3*, 13, https://doi.org/10.1186/s40562-016-0045-4.

Pawłowska, J., Włodarska-Kowalczuk, M., Zajączkowski, M., Nygård, H. & Berge, J. 2011: Seasonal variability of meio- and macrobenthic standing stocks and diversity in an Arctic fjord (Adventfjorden, Spitsbergen). *Polar Biology 34*, 833–845.

Quadfasel, D., Rudels, B. & Kurz, K. 1988: Outflow of dense water from a Svalbard fjord into the Fram Strait. *Deep Sea Research Part A, Oceanographic Research Papers 35*, 1143–1150.

R Core Team 2020: *R: a language and environment for statistical computing*. R Foundation for Statistical Computing, Vienna, Austria. https://www.R-project.org/.

Rasmussen, T. L. & Thomsen, E. 2014: Brine formation in relation to climate changes and ice retreat during the last 15,000 years in Storfjorden, Svalbard, 76–78°N. *Paleoceanography 29*, 911–929.

Rasmussen, T. L. & Thomsen, E. 2015: Palaeoceanographic development in Storfjorden, Svalbard, during the deglaciation and Holocene: Evidence from benthic foraminiferal records. *Boreas 44*, 24–44.

Ribeiro, S., Limoges, A., Massé, G., Johansen, K. L., Colgan, W., Weckström, K., Jackson, R., Georgiadis, E., Mikkelsen, N., Kuijpers, A., Olsen, J., Olsen, S. M., Nissen, M., Andersen, T. J., Strunk, A., Wetterich, S., Syväranta, J., Henderson, A. C. G., Mackay, H., Taipale, S., Jeppesen, E., Larsen, N. K., Crosta, X., Giraudeau, J., Wengrat, S., Nuttall, M., Grønnow, B., Mosbech, A. & Davidson, T. A. 2021: Vulnerability of the North Water ecosystem to climate change. *Nature Communications 12*, 1–12.

Ribeiro, S., Sejr, M. K., Limoges, A., Heikkilä, M., Andersen, T. J., Tallberg, P., Weckström, K., Husum, K., Forwick, M., Dalsgaard, T., Massé, G., Seidenkrantz, M. S. & Rysgaard, S. 2017: Sea ice and primary production proxies in surface sediments from a High Arctic Greenland fjord: spatial distribution and implications for palaeoenvironmental studies. *Ambio 46*, 106–118.

Rudels, B. & Quadfasel, D. 1991: Convection and deep water formation in the Arctic Ocean-Greenland Sea System. *Journal of Marine Systems 2*, 435–450.

Rysgaard, S., Bendtsen, J., Delille, B., Dieckmann, G. S., Glud, R. N., Kennedy, H., Mortensen, J., Papadimitriou, S., Thomas, D. N. & Tison, J. L. 2011: Sea ice contribution to the air-sea CO_2 exchange in the Arctic and Southern Oceans. *Tellus, Series B: Chemical and Physical Meteorology 63*, 823–830.

Sanchez-Cabeza, J. A. & Ruiz-Fernández, A. C. 2012: ^{210}Pb sediment radiochronology: an integrated formulation and classification of dating models. *Geochimica et Cosmochimica Acta 82*, 183–200.

Schmidt, S., Tronczynski, J., Guiot, N. & Lefevre, I. 2005: Dating of sediments in the Biscay bay: implication for pollution chronology. *Radioprotection 40*, S655–S660.

Schönfeld, J., Alve, E., Geslin, E., Jorissen, F., Korsun, S., Spezzaferri, S. & the Fobimo members 2012: The FOBIMO (FOraminiferal BIoMOnitoring) initiative—Towards a standardised protocol for soft-bottom benthic foraminiferal monitoring studies. *Marine Micropaleontology 94-95*, 1–13.

Schröder, C. J. 1988: Subsurface preservation of agglutinated foraminifera in the northerst atlantic ocean. *Abhandlungen der Geologischen Bundesanstalt 41*, 325–336.

Seidenkrantz, M. S. 2013: Benthic foraminifera as palaeo sea-ice indicators in the subarctic realm - examples from the Labrador Sea-Baffin Bay region. *Quaternary Science Reviews 79*, 135–144.

Silverberg, N., Nguyen, H. V., Delibrias, G., Koide, M., Sundby, B., Yokoyama, Y. & Chesselet, R. 1986: Radionuclide profiles, sedimentation rates, and bioturbation in modern sediments of the Laurentian Trough, Gulf of St. Lawrence. *Oceanologica Acta 9*, 285–290.

Skogseth, R., Fer, I. & Haugan, P. M. 2005a: Dense-water production and overflow from an arctic coastal polynya in Storfjorden. *Geophysical Monograph Series 158*, 73–88.

Skogseth, R., Haugan, P. M. & Haarpaintner, J. 2004: Ice and brine production in Storfjorden from four winters of satellite and in situ observations and modeling. *Journal of Geophysical Research C: Oceans 109*, 1–15.

Skogseth, R., Haugan, P. M. & Jakobsson, M. 2005b: Watermass transformations in Storfjorden. *Continental Shelf Research 25*, 667–695.

Skogseth, R., Smedsrud, L. H., Nilsen, F. & Fer, I. 2008: Observations of hydrography and downflow of brine-enriched shelf water in Storfjorden polynya, Svalbard. *Journal of Geophysical Research: Oceans 113*, 1–13.

Smedsrud, L. H., Budgell, W. P., Jenkins, A. D. & Ådlandsvik, B. 2006: Fine-scale sea-ice modelling of Storfjorden polynya, Svalbard. *Annals of Glaciology 44*, 73–79.

Smith, W. Jr & Barber, D. G. 2007: *Polynyas: Windows to the World*. 474 pp. Elsevier, Amsterdam.

Szymańska, N., Pawłowska, J., Kucharska, M., Kujawa, A., Łącka, M. & Zajączkowski, M. 2017: Impact of shelf-transformed waters (STW) on foraminiferal assemblages in the outwash and glacial fjords of Adventfjorden and Hornsund, Svalbard. *Oceanologia 59*, 525–540.

Tomašových, A., Kidwell, S. M., Alexander, C. R. & Kaufman, D. S. 2019: Millennial-scale age offsets within fossil assemblages: result of bioturbation below the taphonomic active zone and out-of-phase production. *Paleoceanography and Paleoclimatology 34*, 954–977.

de Vernal, A., Gersonde, R., Goosse, H., Seidenkrantz, M. S. & Wolff, E. W. 2013: Sea ice in the paleoclimate system: the challenge of reconstructing sea ice from proxies - an introduction. *Quaternary Science Reviews 79*, 1–8.

Vihtakari, M. 2020: *PlotSvalbard - Plot research data from Svalbard on maps*. R package version 0.9.2. https://github.com/MikkoVihtakari/PlotSvalbard.

Vincent, R. F. 2019: A study of the North Water polynya ice arch using four decades of satellite data. *Scientific Reports 9*, 20278, https://doi.org/10.1038/s41598-019-56780-6.

Supporting Information

Additional Supporting Information to this article is available at http://www.boreas.dk.

Fig. S1. Benthic foraminiferal accumulation rates (BFAR) expressed as number of individuals per cm^2 per year, calculated on (A) total (living + dead, 0–1 cm) and (B, C) fossil faunas (3–4 and 6–8 cm).

Table S1. Densities of fossil foraminifera from the 3–4 and 6–8 cm layers (>150-μm size fraction) normalized for 50 cm^3 of volume.

Table S2. Densities of dead foraminifera from the 0–1 cm layer (>150-μm size fraction) normalized for 50 cm^3 of volume.

Table S3. Taxonomic list of the foraminiferal species cited in the study.